

Immobilized cultivation of the red macroalga *Ochtodes secundiramea* via fluid injection of clonal shoot tissues onto porous mesh panels

Joseph A. Kraai* and Gregory L. Rorrer

School of Chemical, Biological, and Environmental Engineering, Oregon State University,
Corvallis, Oregon, 97331 USA

*corresponding author, kraaij@oregonstate.edu

Abstract

This study investigated the feasibility of cultivating clonal red macroalgae on a porous mesh support. Clonal plantlets of macrophytic red alga *Ochtodes secundiramea* served as the model culture system. The morphology of *O. secundiramea* is defined by highly-branched shoot tissues. Plantlets were mechanically blended (8000 rpm, 7 s) and allowed to recover for 7 days prior to immobilization. A 2.0 g FW L⁻¹ slurry of 3 mm branched shoot tissues was injected at onto a fiberglass mesh with 1.6 mm openings in 0.5 s bursts at pressure of 8 bar and nominal fluid velocity of 1.7 m s⁻¹. Each burst deposited a 25 mg shoot tissue cluster onto the mesh. Clusters were placed on a rectangular pitch at decreasing intervals of 20, 12, 8, and 6 mm (contiguous layer) in order to increase the inoculation density. A parallel array of upright, plantlet-inoculated mesh panels was positioned at the base of an aerated, externally illuminated tank, and enriched artificial seawater medium flowed across both sides of each panel. Biomass growth was linear with time, and increased by a factor of 10 over the 28 day cultivation period. Increasing panel inoculation density from 49 to 114 g FW m⁻² panel mesh area doubled panel biomass productivity from 14.5 to 28.6 g FW m⁻² day⁻¹. Immobilized plantlets proliferated outward across the mesh surface to form a highly branched, densified shoot tissue mass about 1.5 cm thick, and final panel biomass coverage exceeding 3.0 kg FW per m² of active panel area was achieved. Overall, the outcomes of this study demonstrate that pressurized fluid injection of clonal plantlets onto a mesh surface, and the subsequent proliferation of the shoot tissues on the mesh to form a contiguous panel, offers potential for the future automation and intensification of red macroalgal biomass production.

Keywords: clonal, immobilization, red macroalgae, shoot, tissue

1. Introduction

Macroalgae (seaweeds) have significant commercial importance [1] and future potential to address global sustainability issues, including carbon sequestration [2–5], waste water treatment [6,7], and renewable feed stocks for fuels and chemicals [8,9]. Red macroalgae (phylum Rhodophyta) are of particular interest for human food, animal feed, and phycocolloid production [10,11]. For example, red macroalgae in genera *Kappaphycus* and *Eucheuma* account for over 80% of global carrageenan production, while *Gracilaria* red algae are responsible for over 60% of global agar production [11]. Some species of *Gracilaria* and *Kappaphycus* are rich in polysaccharides that can be fractionated for subsequent conversion to biofuels and value-added bioproducts [12,13]. Macrophytic red algae within family Rhizophyllidaceae, particularly *Ochtodes secundiramea* and *Portieria hornemannii*, produce monoterpenes with potential applications in bioactive compound development and feed stocks for advanced hydrocarbon biofuels [14–17].

Current practices for scalable cultivation of red macroalgae have well-known limitations. Open water rope-line cultivation of red macroalgae requires labor intensive practices for hatchery operations, inoculation, and harvesting processes [18,19]. Although land-based aerated tank culture of red macroalgae has potential for intensification of biomass production [20], the productivity of aerated tumbler tanks is often limited by the excessive aeration requirements needed to suspend the biomass. This can lead to high aeration costs and limit biomass densities to 10 to 15 grams of fresh weight per liter [21].

New approaches are needed to intensify the production of red macroalgae in engineered systems. These approaches are enabled through clonal propagation. Cell and tissue culture techniques can be used to clonally propagate red macroalgae that possess terete shoot tissue morphology [22]. For example, in our previous work, clonal shoot tissue cultures have been developed for *Agardhiella subulata* [23], *Ochtodes secundiramea* [24], and *Portieria hornemannii* [17] using callus induction and shoot tissue regeneration techniques. These shoot tissues are propagated by cutting the parent shoot tissue into fragments, causing new shoot growth to symmetrically emanate from the cut fragments, creating highly branched plantlets.

The goal of this study is to investigate the feasibility of cultivating clonal red macroalgae on a porous mesh support as a future platform for intensifying engineered production of biomass in scalable cultivation systems. The macrophytic red alga *Ochtodes secundiramea* was selected to

serve as the model organism for this purpose. The densely branched morphology of *O. secundiramea* clonal shoot tissue makes it amenable to attachment onto a porous substrate. Pressurized fluid injection of red macroalgae clonal shoot tissues into a porous mesh panel may provide a simplified mode of inoculation with greater potential for automation. Furthermore, cultivation of macroalgae immobilized on stationary panels may enable process intensification by uncoupling aeration from mixing and enabling improved control of hydrodynamic conditions and nutrient transfer at the stationary biomass surface.

Below, we describe the immobilization and cultivation of *O. secundiramea* clonal shoot tissues onto a mesh panel. The algae panel is cultivated in artificial seawater medium with fluid flow circulating over both sides of the panel. The effects of panel inoculation density on biomass productivity and tissue morphology provide insights into how *O. secundiramea* plantlets grow and proliferate when immobilized onto a stationary porous surface.

2. Materials and methods

2.1 O. secundiramea tissue culture maintenance

Clonal shoot tissues (plantlets) of the tropical marine red macroalga *Ochtodes secundiramea* (Montagne) Howe (Crytonemiales, Rhizophyllidaceae) were developed via callus induction and shoot regeneration as described in our previous work [24]. Plantlets were grown in Instant Ocean artificial seawater medium (30 ppt salinity) enriched with 8X modified Guillard's f/2 enrichment nutrients [25] at pH 8.0 in 500 mL bubbler flasks. Guillard's f/2 nutrients include 0.88 mM nitrate and 0.036 mM phosphate. Stock cultures were maintained at an incident light intensity of 200 $\mu\text{mol m}^{-2} \text{s}^{-1}$ on a 14 h:10 h light:dark photoperiod. Plantlets were sub-cultured every 42 days by mechanically cutting shoot tissues into nominally 1 to 3 mm fragments in a Waring MX1300XTX blender (8000 rpm, 7 s). An aliquot of the blended shoot tissue slurry (typically 20 mL) was inoculated into 400 mL of artificial seawater medium to an initial density of approximately 1 g FW L⁻¹. Typical biomass density and plantlet size after a 42 day cultivation time were approximately 20 g fresh weight (FW) L⁻¹ and 10 mm, respectively. All cultivation and culture handling processes were carried out at 22 °C.

2.2 Preparation of shoot tissues for panel inoculation

An 18 g FW aliquot of shoot tissue biomass was collected from pooled 42 day old *O. secundiramea* bubbler flask cultures and washed with 1.0 L of artificial seawater medium (30 ppt

Instant Ocean[®] with 8X Guillard's f/2 enrichment nutrients). The washed biomass was re-suspended in 1.5 L artificial seawater medium, and blended in a Waring MX1300XTX blender at 8,000 rpm for 7 s. The blended biomass was collected by vacuum filtration on a Büchner funnel.

Blended plantlet fragments were conditioned by aerated tumble culture with periodic filtration of the biomass suspension to remove blending-induced detritus. A 3.8 L glass vessel (25.4 cm height, 15.2 cm inner diameter) was filled with 3.0 L fresh artificial seawater medium enriched with Guillard's 8f nutrient supplement adjusted to pH 8.5, and inoculated with blended plantlets to initial biomass density of 5 g FW L⁻¹. Cultivation conditions for the shoot tissue fragment conditioning process are presented in Table 1. House air was sterilized with an inline filter (0.5 µm), humidified, and bubbled into the bottom of the vessel through a fine-bubble diffuser at 1.2 L min⁻¹. Overhead illumination on a 14 h:10 h light:dark photoperiod was supplied by a Viparspectra DS300 adjustable power 300 W Light-Emitting Diode (LED) array. The incident light intensity was set to 800 µmol m⁻² s⁻¹ at the liquid surface. The conditioning process proceeded for 7 days, with daily filtration of the plantlet suspension (Whatman No. 1, pore size 11 µm) to remove detritus from viable shoot tissue. After filtration, viable plantlets were weighed, imaged, and then immediately returned to the cultivation tank with the filtered medium. After the final filtration step, the plantlet suspension was screened through 6 mm mesh. The screened plantlets were collected by vacuum filtration on a Büchner funnel, washed with 500 mL of fresh medium, and then re-suspended in fresh medium.

2.3 Immobilization of shoot tissues onto mesh panel surface

Mesh panels were prepared by cutting fiberglass mesh sheet (1.6 mm openings, 0.3 mm nominal wire thickness) into 7.0 cm squares. The cut mesh was surface sterilized with 5% sodium hypochlorite bleach, then 70% ethanol. The device shown in Fig. 1 was used to immobilize blended *O. secundiramea* plantlets into a mesh panel by a pressurized fluid injection process. Typically, 500 mL of artificial seawater medium containing 2 g FW L⁻¹ conditioned *O. secundiramea* plantlets was loaded into the re-sealable pressurized chamber (5 cm inner diameter, 1200 mL total volume). Compressed N₂ gas was bubbled to the bottom of the chamber to mix the plantlet suspension and pressurize the chamber headspace to nominally 8.0 bar. The injector nozzle had an inner diameter of 6 mm, and was surrounded by a 10 mm skirt to deflect scattered fluid flow back onto the mesh. The pressurized plantlet suspension was injected through a ball valve onto the mesh in 0.5 s bursts, embedding the shoots into the mesh openings.

Typically, one 0.5 s burst was required to reproducibly inject a cluster of 25 mg FW plantlets onto the mesh. Periodically, the pressure relief valve was briefly opened and closed to re-mix and pressurize the plantlet suspension. The fluid injection velocity was experimentally determined by measuring the volume dispensed from the nozzle over time. The critical injection velocity, defined as the minimum fluid velocity required for retention of immobilized plantlets on the mesh, was nominally 1.7 m s^{-1} .

Panel inoculation density was controlled by manipulating the pitch (spacing) between injected plantlet clusters. Three replicate panels of four different inoculation densities were prepared: clusters at 20 mm square pitch; clusters at 12 mm square pitch; adjacent plantlet clusters at 8 mm square pitch, where the rims of plantlet clusters touched; and clusters of nominal 6 mm pitch, which overlapped to provide a contiguous layer of plantlets. Plantlets injected onto a mesh with 1 mm openings rested on top surface of the mesh, whereas injection of plantlets onto mesh with 3 mm openings completely passed through mesh. Thus, the mesh with 1.6 mm openings was optimal for immobilization of the *O. secundiramea* clonal shoot tissues.

2.4 Shoot tissue cultivation on mesh panel

The cultivation system is shown in Fig. 2. The inoculated mesh panels were vertically mounted on modular support frames. A single panel frame module held two panels. The total module frame height was 18 cm. Six panel frame modules (12 total panels, 3 panels at each inoculation density, total initial biomass of 3.928 g FW) were placed 5.1 cm apart at the bottom of a 20 L rectangular cultivation tank (length 32.6 cm, width 25.4 cm, depth 25.4 cm). The cultivation conditions are presented in Table 1. The 20 L tank was filled to a level of 20 cm with 16.5 L of artificial seawater medium containing 8X Guillard's *f/2* enriched nutrients (6.7 mM nitrate), adjusted to pH 8.5. House air was sterilized with an inline filter ($0.5 \mu\text{m}$), humidified, and bubbled into the bottom edge of the tank at a rate of $5 \text{ L}^{-1} \text{ min}$ ($0.30 \text{ L air L}^{-1} \text{ liquid min}^{-1}$) through fine-bubble tube diffuser to provide a CO_2 delivery rate of $0.30 \text{ mmol CO}_2 \text{ L}^{-1} \text{ h}^{-1}$. The air bubbles rose up the wall of the tank and generated a circulating flow pattern with an approximate fluid velocity of 10 cm s^{-1} at the liquid surface, as determined by the timing the linear motion of float across the surface of the tank. The upright panel surfaces were aligned parallel to the direction of the circulating flow. A Viparspectra DS300 adjustable power 300W LED array supplied overhead illumination. The incident light intensity at the liquid surface was set to $1000 \mu\text{mol m}^{-2} \text{ s}^{-1}$, and the photoperiod was 14 h: 10 h light: dark. A 3400X stock solution

of Guillard's *f/2* nutrient was fed at 0.58 mL day^{-1} to the cultivation medium to provide an equivalent nutrient delivery rate of $0.12 \text{ mmol N L}^{-1} \text{ day}^{-1}$, where N is based on nitrate. Nutrient delivery was sufficient to avoid nutrient limitation based on our previous work [15]. The plantlet size and biomass fresh weight were measured every 3 to 4 days.

2.5 Aerated tumble culture

Conditioned *O. secundiramea* plantlets were cultivated within the aerated tumble culture tank described earlier in section 2.2. The cultivation conditions were similar to panel cultivation (Table 1). The initial nutrient concentration was 8X Guillard's *f/2* (6.7 mM nitrate). The tumble culture vessel was inoculated to initial density of 1.0 g FW L^{-1} and fed 0.44 mL day^{-1} of 3400X stock solution of Guillard's *f/2* nutrients to provide an equivalent rate of $0.5 \text{ mmol N L}^{-1} \text{ day}^{-1}$, where N is based on nitrate. At the initial biomass density of 1.0 g FW L^{-1} , nutrient delivery was sufficient to avoid nutrient limitation based on our previous work [15]. The plantlet size and biomass fresh weight were measured every 3 to 4 days. The plantlets were suspended in tumble culture throughout the 28 day cultivation period.

2.6 Biomass measurements

Prior to fresh biomass weight measurement, shoot tissues on the panel mesh were patted dry with a paper towel. Tumble culture plantlets were dewatered and rinsed with distilled water under suction for 30 s in a Büchner funnel lined with Whatman No. 1 filter paper. Biomass samples were rinsed in distilled water to remove surface salts, weighed, dried at $80 \text{ }^{\circ}\text{C}$ for 18 h, and weighed again to determine dry weight (DW) content. The ash-free dry weight (AFDW) of dried biomass samples was determined by loss after heating at $550 \text{ }^{\circ}\text{C}$ for 10 h in a muffle furnace. All assays were performed in triplicate.

2.7 Imaging

Images of the shoot tissues on the mesh panel and tumble-cultured plantlets were captured with a 12 megapixel camera. Images were imported to *ImageJ* software (National Institutes of Health) and converted to 8-bit format with threshold to improve contrast. The mean diameter and area of individual plantlets or plantlet clusters were estimated by fitting an ellipse to the threshold image element. For a contiguous layer of plantlets on the mesh, the biomass perimeter was manually selected. The active area was defined as the total area occupied by the biomass on the panel. The fractional coverage of biomass immobilized on a given panel was determined by dividing the active area by the area of the final biomass boundary after a 28 day cultivation

time. An image of each panel cross section was also captured to determine mean thickness of the biomass layer.

2.8 Photosynthesis-irradiance measurements

The specific photosynthetic oxygen evolution rate (OER) vs. irradiance curve for *O. secundiramea* plantlets was determined using methods adapted from previous work [26]. These measurements were fitted to data to a photosynthesis-irradiance (*P-I*) model of the form

$$P_o = Q_o + P_{o,max} \left(1 - e^{-\frac{I}{I_k}} \right) \quad (1)$$

by nonlinear, least-squares regression using the Marquardt method, where *I* is the irradiance (400-700 nm photosynthetically active range, $\mu\text{mol photons m}^{-2} \text{ s}^{-1}$); Q_o the specific respiration rate measured in the dark ($\text{mmol O}_2 \text{ g}^{-1} \text{ DW h}^{-1}$); P_o is the net specific oxygen evolution rate at a given irradiance ($\text{mmol O}_2 \text{ g}^{-1} \text{ DW h}^{-1}$); $P_{o,max}$ ($\text{mmol O}_2 \text{ g}^{-1} \text{ DW h}^{-1}$) is the specific oxygen evolution rate at light saturation; and I_k ($\mu\text{mol m}^{-2} \text{ s}^{-1}$) is the irradiance at 62.3% of light saturation.

2.9 Statistical analysis of data

All experimental measurements and analyses were repeated in duplicate or triplicate, with point standard deviations (1.0 S.D.) or standard errors (1.0 S.E.) reported. Biomass production rate on a panel was determined by least-squares linear regression of experimental biomass on panel vs. time data with slope error reported as 1.0 S.E. *P-I* model parameters Q_o , $P_{o,max}$, and I_k were estimated by fitting experimental P_o vs. *I* data to Equation 1 via nonlinear, least-squares regression (Marquardt method) using Statgraphics Centurion XVII software, with coefficient errors reported as 1.0 S.E. One-way analysis of variance (ANOVA) was used to assess the statistical significance of difference in net specific oxygen evolution rate ($P_o - Q_o$) of *O. secundiramea* tissue blended at different speeds.

3. Results

3.1 Conditioning of shoot tissues before immobilization

Flask cultured *O. secundiramea* plantlets were blended in a Waring blender for 7 s at 8000 rpm. Blended shoot tissue fragments (microplantlets) of *O. secundiramea* shoot tissues, nominally 1-2 mm in size, were conditioned in aerated tumble culture tanks for 7 days, with daily filtration of the biomass suspension to remove detritus generated by the blending process.

Biomass growth and photosynthetic oxygen evolution rate for the conditioning phase are presented in Fig. 3. The biomass density decreased by 30% during the first day of conditioning, followed by a steady increase through day 7 (Fig. 3a). The initial decrease in biomass density was attributed to detritus formation resulting from tissue blending. Over the 7 day conditioning phase, successive daily filtrations of the biomass suspension eliminated visible detritus from the viable tissue. Biomass density increased by 36%, and mean plantlet diameter doubled from 1.4 to 2.8 mm. Immediately after blending, the specific oxygen evolution rate (P_o) of plantlet tissue decreased by 36%. After 7 days of the conditioning cultivation, the P_o of the blended tissue increased back to the value of the shoot tissue before it was blended, indicating that the tissue recovered from the blending process (Fig. 3b).

The effect of blending speed on Q_o and P_o immediately after the blending process is presented in Fig. 4. The specific respiration rate (Q_o) increased with blending speed. However, there was no statistical difference in net specific oxygen evolution rate ($P_o - Q_o$) at blending speeds ranging from 8,000 to 20,000 rpm ($p = 0.692$, 95% confidence).

3.2 Photosynthesis-irradiance curve

The photosynthesis-irradiance ($P-I$) curve for *Ochtodes secundiramea* plantlets is presented in Fig. 5. The data were fitted to Equation (1) by nonlinear, least-squares regression, with $Q_o = -0.069 \pm 0.011$ mmol O₂ g⁻¹ DW h⁻¹, $P_{o,max} = 0.24 \pm 0.012$ mmol O₂ g⁻¹ DW h⁻¹, and $I_k = 63 \pm 8$ μmol m⁻² s⁻¹. All reported errors are ± 1.0 standard error (S.E.). At the cultivation light intensity of 1000 μmol m⁻² s⁻¹, or OER measurements of 300 μmol m⁻² s⁻¹, the photosynthetic activity relative to light saturation, defined as $(P_o - Q_o)/P_{o,max}$, was greater than 99%.

3.3 Fluid injection of plantlets into mesh panel

The device shown in Fig. 1 deposited the conditioned *O. secundiramea* shoot tissues of 2-3 mm nominal size into a 7 x 7 cm fiberglass 12 mesh sheet (1.6 mm opening size) by injecting a pressurized slurry of plantlets onto the mesh. A minimum fluid injection velocity of nominally 1.7 m s⁻¹ was required to immobilize plantlet clusters in the slurry (2.0 g FW L⁻¹) into the mesh. Below this velocity, the plantlet slurry lacked the force required to infiltrate the shoot tissues into the 1.6 mm openings. The fluid injection velocity used to immobilize plantlets into the panel for cultivation experiments was 2.5 m s⁻¹.

Selected parameters that characterize the inoculation density of immobilized plantlets directly after fluid injection onto the mesh sheet are presented in Table 2. The inoculation

density on the panel was controlled by varying the number and spacing of plantlet clusters injected onto the mesh. Typically, a single injected cluster of 25 mg FW plantlets had a diameter of 7 mm. Panels with one contiguous layer of injected plantlets had an initial biomass loading of 0.6 g FW per panel. It is noted here that if the blended shoot tissues were not conditioned for 7 days to remove detritus, then the detritus tended to coat the viable shoot tissue and ultimately caused cessation of growth.

3.3. Biomass growth on mesh panel vs. tumble culture

Biomass growth curves for *O. secundiramea* shoots tissues cultivated on the mesh sheet and as freely-suspended plantlets in tumble suspension are compared in Fig. 6. In both cultivation modes, the liquid was aerated and mixed by a rising stream of air bubbles. In the panel cultivation, aeration was introduced along the wall of the cultivation chamber holding the panels to induce flow of liquid across the panel surface (Fig. 2). In panel culture, the biomass growth vs. time profile was linear over the 28 day cultivation period. In tumble culture, biomass growth was nearly exponential for the first 14 days, and then slowed to linear growth during the next 14 days. Shoot tissues immobilized on panels grew about half as fast as shoot tissues suspended in tumble culture. For aerated panel culture, the pH increased from 8.4 to 8.9 over the course of the 28 day cultivation, whereas for tumble culture, the pH increased to 9.3, which is indicative of high CO₂ demand. After 28 days of cultivation, there was no evidence of microalgal contamination associated with the biomass or liquid medium in either aerated tumble cultivation or panel cultivation. At the end of the 28 day cultivation, the biomass attached to the panel could be harvested by raking the shoot tissues from the mesh.

The effects of inoculation density on *O. secundiramea* growth during panel cultivation are presented in Fig. 7. Biomass productivity parameters are summarized in Table 2. Biomass production on the panel increased linearly with time (Fig. 7a). The linear biomass production rate at a given inoculum density was estimated from the least-squares slope of this data. This rate of biomass production increased with increasing inoculation density on the panel (Fig. 7b), where doubling the inoculation density from 49 g FW m⁻² (20 mm spacing between plantlet clusters) to 114 g FW m⁻² (contiguous layer of plantlets) also doubled the linear biomass growth rate from 14.5 ± 0.9 to 28.6 ± 0.5 g FW m⁻² day⁻¹ (1.0 S.E.). This rate is based on the total area of the 7 x 7 cm panel, not the area on this panel where the biomass was actually deposited.

After 28 days of cultivation, the specific oxygen evolution rate (P_o) of the biomass on the panel decreased modestly with increasing inoculation density (Fig. 7c), indicating that densifying the biomass on the mesh reduced the intrinsic growth rate even though the overall linear rate of biomass production increased. Furthermore, the range of P_o values were nominally half those for aerated tumble culture of free plantlets, consistent with the growth curves presented earlier in Fig. 6b. At the end of the cultivation, the dry weight of the biomass was 19.0 ± 0.5 wt% (1.0 S.D., n = 3), and the ash-free dry weight (AFDW) content was 11.1 ± 0.3 wt% (1.0 S.D., n = 3).

3.4 Growth morphology

Representative images of the panels at inoculation and after 28 days of cultivation are presented in Fig. 8, and representative images of the panel cross section (thickness) are presented in Fig. 9. During cultivation, shoot tissues within the plantlet clusters grew outward across the panel area, filled in gaps existing within the porous biomass matrix at inoculation, and increased the overall thickness of the biomass layer on the panel. Individual plantlet clusters on the panel increased from 7.3 to 12.4 mm average diameter, and the thickness of the biomass layer on the panel consistently doubled from 6.4 to 13.0 mm, independent of inoculation density (Table 2). Plantlet clusters inoculated at 12 and 20 mm spacing did not grow together, but adjacent clusters at 8 mm nominal spacing ultimately grew into a contiguous layer. Generally, the shoot tissues proliferated more extensively on the panel side that was inoculated by pressured fluid injection. Plantlets suspended in tumble culture approximately doubled in diameter from 2.6 to 6.3 mm, with many plantlets exceeding 15 mm. After 28 days, shoot tissues were highly branched relative to the blended, conditioned shoot tissues.

The time course for fractional biomass coverage, based on the outer perimeter of the biomass active zone, and biomass loading per active area for *O. secundiramea* shoot tissues growing on the mesh panel, are compared in Figs. 10a and 10b respectively. In Fig. 10, the active area is defined as the mesh area containing immobilized biomass, not the overall area of the mesh sheet. For example, the active area based on the outer perimeter of the biomass contiguous layer at the end of the cultivation was 28% of the total 7 x 7 cm panel mesh area. The fractional coverage on the panel mesh linearly increased during cultivation. However, the biomass loading per active area increased significantly within the first 21 days and then leveled off from 21 to 28 days, particularly for the contiguous layer inoculation. In the later stage of cultivation, the shoot tissue matrix was filling voids on the surface and extending the perimeter of the active area.

Based on the active area, biomass loadings exceeding 3000 g FW m⁻² were obtained for the contiguous layer inoculation process after 28 days of cultivation.

4. Discussion

O. secundiramea was chosen as a model system to illustrate the potential of immobilizing shoot tissues of clonal red macroalgae onto mesh support. This support enabled the growing biomass to become densely compacted onto a stationary surface. The stationary macroalgae panels can be modularly deployed into any cultivation system. The immobilization process developed in this study could potentially be adapted to other macrophytic red algae that can be clonally propagated, and possess a branched shoot tissue morphology, such as *Gracilaria*, *Eucheuma*, and *Kappaphycus* species [27].

This study demonstrated that clonal plantlets of *O. secundiramea* can be deposited onto a porous mesh sheet in a controlled manner by pressurized fluid injection of a plantlet suspension onto the mesh surface. For blended plantlets of 2-3 mm nominal size, a 2 g FW L⁻¹ plantlet suspension with velocity of at least 1.7 m s⁻¹ was required to secure the shoot tissues to a mesh surface with 1.6 mm openings. The highly-branched morphology of the *O. secundiramea* shoot tissues made this alga particularly amenable to entanglement with the porous mesh. Prior to immobilization, plantlets were blended into shoot tissue fragments, and then conditioned in aerated tumble culture with daily filtration of the culture suspension to remove detritus from the blending process. The shoot tissue inoculation density was controlled by varying the spacing between injected plantlet clusters, ranging from 20 mm rectangular pitch to a contiguous layer of plantlets, and biomass production rate on the mesh surface scaled to the inoculum density.

The fluid injection process used to immobilize clonal shoot tissues of macrophytic red algae into the mesh panel can potentially be scaled and automated. For example, a manifold or array of injector nozzles could be used to accommodate a variety of panel dimensions, mesh sizes, and plantlet morphologies. Automation may be achieved through the incorporation of mechanized systems such as an actuated injector valve and a mesh panel conveyor system.

A potential limitation of this process was the need to remove the detritus from the blended shoot tissue slurry, to avoid its re-attachment to the shoot tissues during the inoculation process. This may be the consequence of very small shoot tissue fragments generated from blending of the fine shoot structures characteristic of *O. secundiramea*. Other red macroalgae with larger

shoot structures may not be subject to this limitation, and consideration of these other organisms will be reserved for future work.

The panels were mounted on modular support frames, and deployed within an illuminated cultivation tank to assess growth performance. A rising stream of air bubbles provided mixing and gas exchange, and promoted fluid flow over the stationary panel surface. The cultivation conditions were designed to be replete with respect to light, CO₂, and macronutrient delivery. Plantlets immobilized on the panel grew into a highly branched, densified mass of shoot tissues. Initially the shoot tissues spread out over the panel surface, and then grew outward from the panel surface, ultimately carpeting the mesh with a dense shoot tissue layer that was about 1.5 cm thick. The maximum biomass coverage exceeded 3000 g FW m⁻² after 28 days of cultivation.

Biomass production on the mesh panel increased linearly with time. A linear growth profile under nutrient replete conditions suggests other processes were limiting the growth rate of the shoot tissues imbedded into the mesh panel. Boundary layer flow of seawater over the surface of macroalgae tissue surfaces is known to influence the rate of dissolved nutrient transfer to the biomass, particularly in low flow velocity environments [28,29]. Reduced flow of fluid through the densified biomass matrix near the panel surface may have hindered nutrient transfer to the immobilized shoot tissues. In this context, it is suggested that the freely-suspended plantlets may have grown faster in aerated tumble tank culture because of increased intensity of fluid-tissue interaction.

The cultivation of red macroalgae immobilized on mesh panels offers two opportunities for process intensification. First, aeration can be uncoupled from mixing, reducing the total aeration requirement and enabling greater control of fluid velocity over the immobilized tissue, a key determinant of nutrient uptake and biomass growth [28,29]. Second, areal biomass productivity can be intensified. The *O. secundiramea* tissue grew as a compact, densified biomass layer on the panel surface up to about 1.5 cm thick. The dense tissue mass on the panel would enable vertically hung panels to be spaced closely spaced together parallel to the direction of fluid flow, with illumination directed at the liquid surface, as shown in Fig. 2.

To provide an example of process intensification, if the biomass is inoculated over the entire panel surface area (A), and not just the active area (A_p), then the growth rate on the *panel surface area* is scaled by

$$R_{X,p} = R_X (A / A_p) \quad (2)$$

where $R_X = 28.6 \text{ g FW m}^{-2} \text{ day}^{-1}$ and $A_p / A = 0.28$ for the contiguous layer (Table 2), yielding $R_{X,p} = 102 \text{ g FW m}^{-2} \text{ day}^{-1}$. In this context, consider a scenario where mesh panels are inoculated with a contiguous layer of plantlets to 400 g FW m^{-2} panel area, spaced 5.0 cm apart to allow for flow between the panels and across the surface of shoot tissue emanating from the panel. These panels are extended to a vertical dimension of 20 cm , typical for the depth of an open raceway pond. Based on these conditions, the estimated final biomass density would be 62 g FW L^{-1} ($6.8 \text{ g AFDW L}^{-1}$) after 28 days of cultivation, and the estimated *areal* productivity would be $389 \text{ g FW m}^{-2} \text{ day}^{-1}$ ($43 \text{ g AFDW m}^{-2} \text{ day}^{-1}$), comparable to the higher productivity range of microalgae cultivation [30].

Given that high areal productivities are possible, in future work, the *O. secundiramea* panels described here will be cultivated in a circular raceway channel, where fluid of a defined velocity field will interact with the dense mat of shoot tissue proliferating from the mesh surface. This information will be used to suggest strategies for continued process intensification of red macroalgae panel cultivation in scalable, engineered cultivation systems.

Declaration of authors' agreement

All authors agree to the authorship and submission of the manuscript to *Algal Research* for peer review.

Authorship Contribution Statement

J. Kraai and G. Rorrer designed the experiments. J. Kraai performed the experimental work. J. Kraai and G. Rorrer prepared the manuscript.

Declaration of competing interest

The authors declare no conflicts of interest.

Declaration of informed consent, Human/Animal Rights

No conflicts, informed consent, or human or animal rights are applicable to this study.

Acknowledgements

This work was supported through the National Aquaculture Initiative of the U.S. National Oceanographic and Atmospheric Administration (NOAA), administered through the National Sea Grant Program under award number NA18OAR4170328.

References

- [1] A.H. Buschmann, C. Camus, J. Infante, A. Neori, Á. Israel, M.C. Hernández-González, S. V. Pereda, J.L. Gomez-Pinchetti, A. Golberg, N. Tadmor-Shalev, A.T. Critchley, Seaweed production: overview of the global state of exploitation, farming and emerging research activity, *Eur. J. Phycol.* 52 (2017) 391–406. doi:10.1080/09670262.2017.1365175.
- [2] D. Krause-Jensen, C.M. Duarte, Substantial role of macroalgae in marine carbon sequestration, *Nat. Geosci.* 9 (2016) 737–742. doi:10.1038/ngeo2790.
- [3] C.M. Duarte, J. Wu, X. Xiao, A. Bruhn, D. Krause-Jensen, Can seaweed farming play a role in climate change mitigation and adaptation?, *Front. Mar. Sci.* 4 (2017). doi:10.3389/fmars.2017.00100.
- [4] C.F.A. Sondak, P.O. Ang, J. Beardall, A. Bellgrove, S.M. Boo, G.S. Gerung, C.D. Hepburn, D.D. Hong, Z. Hu, H. Kawai, D. Largo, J.A. Lee, P.E. Lim, J. Mayakun, W.A. Nelson, J.H. Oak, S.M. Phang, D. Sahoo, Y. Peerapornpis, Y. Yang, I.K. Chung, Carbon dioxide mitigation potential of seaweed aquaculture beds (SABs), *J. Appl. Phycol.* 29 (2017) 2363–2373. doi:10.1007/s10811-016-1022-1.
- [5] L.M.L. Laurens, M. Lane, R.S. Nelson, Sustainable Seaweed Biotechnology Solutions for Carbon Capture, Composition, and Deconstruction, *Trends Biotechnol.* 38 (2020) 1232–1244. doi:10.1016/j.tibtech.2020.03.015.
- [6] N. Arumugam, S. Chelliapan, H. Kamyab, S. Thirugnana, N. Othman, N.S. Nasri, Treatment of wastewater using seaweed: A review, *Int. J. Environ. Res. Public Health.* 15 (2018) 1–17. doi:10.3390/ijerph15122851.
- [7] J. Liu, B. Pemberton, J. Lewis, P.J. Scales, G.J.O. Martin, Wastewater treatment using filamentous algae – A review, *Bioresour. Technol.* 298 (2019) 122556. doi:10.1016/j.biortech.2019.122556.
- [8] Y. Lehahn, K.N. Ingle, A. Golberg, Global potential of offshore and shallow waters macroalgal biorefineries to provide for food, chemicals and energy: Feasibility and sustainability, *Algal Res.* 17 (2016) 150–160. doi:10.1016/j.algal.2016.03.031.
- [9] A. Leandro, L. Pereira, A.M.M. Gonçalves, Diverse applications of marine macroalgae, *Mar. Drugs.* 18 (2020) 1–15. doi:10.3390/md18010017.
- [10] S. Nayar, K. Bott, Current status of global cultivated seaweed production and markets, *World Aquac.* 45 (2014) 32–37.
- [11] J.K. Kim, C. Yarish, E.K. Hwang, M. Park, Y. Kim, Seaweed aquaculture: Cultivation technologies, challenges and its ecosystem services, *Algae.* 32 (2017) 1–13. doi:10.4490/algae.2017.32.3.3.
- [12] F. Masarin, F.R.P. Cedeno, E.G.S. Chavez, L.E. De Oliveira, V.C. Gelli, R. Monti, Chemical analysis and biorefinery of red algae *Kappaphycus alvarezii* for efficient production of glucose from residue of carrageenan extraction process, *Biotechnol. Biofuels.* 9 (2016) 1–12. doi:10.1186/s13068-016-0535-9.
- [13] S. Kumar, R. Gupta, G. Kumar, D. Sahoo, R.C. Kuhad, Bioethanol production from

- Gracilaria verrucosa*, a red alga, in a biorefinery approach, *Bioresour. Technol.* 135 (2013) 150–156. doi:10.1016/j.biortech.2012.10.120.
- [14] J.J. Polzin, G.L. Rorrer, D.P. Cheney, Metabolic flux analysis of halogenated monoterpene biosynthesis in microplantlets of the macrophytic red alga *Ochtodes secundiramea*, *Biomol. Eng.* 20 (2003). doi:10.1016/S1389-0344(03)00054-6.
- [15] J.P. Polzin, G.L. Rorrer, Halogenated monoterpene production by microplantlets of the marine red alga *Ochtodes secundiramea* within an airlift photobioreactor under nutrient medium perfusion, *Biotechnol. Bioeng.* 82 (2003) 415–428. doi:10.1002/bit.10588.
- [16] J. Polzin, G.L. Rorrer, Selective production of the acyclic monoterpene β -myrcene by microplantlet suspension cultures of the macrophytic marine red alga *Ochtodes secundiramea* under nutrient perfusion cultivation with bromide-free medium, *Algal Res.* 36 (2018) 159–166. doi:10.1016/j.algal.2018.10.022.
- [17] L.F. Barahona, G.L. Rorrer, Isolation of halogenated monoterpenes from bioreactor-cultured microplantlets of the macrophytic red algae *Ochtodes secundiramea* and *Portieria hornemannii*, *J. Nat. Prod.* 66 (2003) 743–751. doi:10.1021/np0206007.
- [18] C. Halling, G. Aroca, M. Cifuentes, A.H. Buschmann, M. Troell, Comparison of spore inoculated and vegetative propagated cultivation methods of *Gracilaria chilensis* in an integrated seaweed and fish cage culture, *Aquac. Int.* 13 (2005) 409–422. doi:10.1007/s10499-005-6977-x.
- [19] D. Valderrama, J. Cai, N. Hishamunda, N. Ridler, I.C. Neish, A.Q. Hurtado, F.E. Msuya, M. Krishnan, R. Narayanakumar, M. Kronen, D. Robledo, E. Gasca-Leyva, J. Fraga, The Economics of *Kappaphycus* Seaweed Cultivation in Developing Countries: A Comparative Analysis of Farming Systems, *Aquac. Econ. Manag.* 19 (2015) 251–277. doi:10.1080/13657305.2015.1024348.
- [20] B.A. Gadberry, J. Colt, D. Maynard, D.C. Boratyn, K. Webb, R.B. Johnson, G.W. Saunders, R.H. Boyer, Intensive land-based production of red and green macroalgae for human consumption in the pacific northwest: An evaluation of seasonal growth, yield, nutritional composition, and contaminant levels, *Algae.* 33 (2018) 109–125. doi:10.4490/algae.2018.33.2.21.
- [21] B.E. Lapointe, J.H. Ryther, Some aspects of the growth and yield of *Gracilaria tikvahiae* in culture, *Aquaculture.* 15 (1978) 185–193. doi:10.1016/0044-8486(78)90030-3.
- [22] G.L. Rorrer, D.P. Cheney, Bioprocess engineering of cell and tissue cultures for marine seaweeds, *Aquac. Eng.* 32 (2004) 11–41. doi:10.1007/978-1-4615-4753-2_20.
- [23] Y. Huang, S. Maliakal, D.P. Cheney, G.L. Rorrer, Comparison of Development and Photosynthetic Growth for Filament Clumps and Regenerated Microplantlet Cultures of *Agardhiella subulata* (Rhodophyta, Gigartinales), *J. Phycol.* 34 (1998) 893–901. doi:10.1046/j.1529-8817.1998.340893.x.
- [24] S. Maliakal, D.P. Cheney, G.L. Rorrer, Halogenated monoterpene production in regenerated plantlet cultures of *Ochtodes secundiramea* (Rhodophyta, Cryptonemiales), *J. Phycol.* 37 (2001) 1010–1019. doi:10.1046/j.1529-8817.2001.00120.x.

- [25] J.A. Berges, D.J. Franklin, P.J. Harrison, Evolution of an Artificial Seawater Medium: Improvements in Enriched Seawater, Artificial Water Over the Last Two Decades, *J. Phycol.* 37 (2001) 1138–1145. doi:10.1046/j.1529-8817.2001.01052.x.
- [26] Y.M. Huang, G.L. Rorrer, Dynamics of oxygen evolution and biomass production during cultivation of *Agardhiella subulata* microplantlets in a bubble-column photobioreactor under medium perfusion, *Biotechnol. Prog.* 18 (2002) 62–71. doi:10.1021/bp010149u.
- [27] P. Baweja, D. Sahoo, P. García-Jiménez, R.R. Robaina, Review: Seaweed tissue culture as applied to biotechnology: Problems, achievements and prospects, *Phycol. Res.* 57 (2009) 45–58. doi:10.1111/j.1440-1835.2008.00520.x.
- [28] Y. Gonen, E. Kimmel, M. Friedlander, Diffusion Boundary Layer Transport in *Gracilaria Conferta* (Rhodophyta), *J. Phycol.* 31 (1995) 768–773. doi:10.1111/j.0022-3646.1995.00768.x.
- [29] C.L. Hurd, Water motion, marine macroalgal physiology, and production, *J. Phycol.* 36 (2000) 453–472. doi:10.1046/j.1529-8817.2000.99139.x.
- [30] R. Davis, J. Markham, C. Kinchin, N. Grundl, E.C.D. Tan, D. Humbird, *Process Design and Economics for the Production of Algal Biomass: Algal Biomass Production in Open Pond Systems and Processing Through Dewatering for Downstream Conversion*, Golden, CO (United States), 2016. doi:10.2172/1239893.

Table 1 Cultivation conditions

Parameter & units	Conditioning	Tumble	Panel
Working volume (L)	3.0	3.0	16.5
Liquid depth (cm)	20	20	20
Temperature (°C)	22	22	22
Incident light intensity at liquid surface, I_0 ($\mu\text{mol m}^{-2} \text{s}^{-1}$)	800	800	1000
Photoperiod (h ON / h OFF)	14:10	14:10	14:10
Aeration rate (L air L ⁻¹ culture min ⁻¹)	0.40	0.40	0.30
Initial biomass loading per unit culture volume (g FW L ⁻¹)	5.1	1.0	0.24
Initial bicarbonate concentration (mM)	2.0	2.0	2.0
Initial nitrate concentration (mM)	14.1	6.7	6.7

Table 2 Summary of biomass loading on mesh support at inoculation and after 28 days of cultivation. All errors are ± 1.0 S.E. (n = 3).

Biomass on Panel	20 mm pitch	12 mm pitch	adjacent 8 mm pitch	contiguous layer < 6 mm pitch
Number of clusters	9	9	16	1
Initial cluster diameter (mm)	8.0 \pm 0.3	7.2 \pm 0.3	6.8 \pm 0.3	7.1 \pm 0.2
Final cluster diameter (mm)	12.2 \pm 0.4	12.5 \pm 0.6	37.2 \pm 2.0	41.8 \pm 1.3
Initial biomass on panel (g FW m ⁻² panel)	49 \pm 0.7	43 \pm 3	62 \pm 5	114 \pm 8
Final biomass on panel (g FW m ⁻² panel)	461 \pm 49	519 \pm 16	604 \pm 84	884 \pm 130
Biomass production rate on panel, R_x (g FW m ⁻² panel day ⁻¹)	14.5 \pm 0.9	16.9 \pm 0.6	19.8 \pm 0.7	28.6 \pm 0.5
Final cluster thickness (mm)	13.0 \pm 0.5	11.1 \pm 1.1	13.1 \pm 0.3	14.9 \pm 0.4
Initial biomass coverage (% active area)	14 \pm 1	18 \pm 1	37 \pm 3	75 \pm 2
Final biomass coverage (% active area)	34 \pm 2	55 \pm 4	69 \pm 3	100 \pm 0
Final biomass on active area (g FW m ⁻²)	2101 \pm 92	2255 \pm 224	2684 \pm 109	3125 \pm 273

Figure Legends

Fig. 1. Pressurized injection of the microplantlet tissue slurry onto the mesh surface.

Fig. 2. Aerated tank for cultivation of vertically-aligned mesh panels. Aeration provided fluid motion over panel surface.

Fig. 3. Conditioning of blended microplantlets. (a) Normalized biomass production (X/X_o) and mean plantlet diameter of *O. secundiramea* plantlets vs. time after blending, where X_o is the initial biomass density (g FW L⁻¹) and X is the current biomass density (g FW L⁻¹). (b) Specific O₂ evolution rate (OER, mmol O₂ g DW h⁻¹), measured at 300 μmol m⁻² s⁻¹ incident light intensity. Errors shown are ± 1.0 S.D., n = 2.

Fig. 4. Effect of blending speed on OER for *O. secundiramea* microplantlets, measured at 300 μmol m⁻² s⁻¹ incident light intensity immediately after blending for 7 s. Errors shown are ± 1.0 S.D., n = 2.

Fig. 5. OER vs. irradiance curve for *O. secundiramea* plantlets. Solid line is best fit to exponential model defined by Equation (1). PAR refers to photosynthetic active radiance (400-700 nm). Errors shown are ± 1.0 S.D., n = 2.

Fig. 6. Biomass production vs. time for *O. secundiramea* plantlets in aerated panel vs. tumble culture. (a) Biomass density (X) and mean plantlet size vs. time in aerated tumble culture. (b) Normalized biomass production (X/X_o) vs. time for aerated tumble culture and mesh panels at four inoculation levels. Errors shown are ± 1.0 S.E., n = 3.

Fig. 7. *Ochtodes secundiramea* plantlet growth on mesh panel vs. initial biomass loading. (a) Biomass per total mesh surface area vs. time. Solid lines represent best fit to linear regression model. (b) Biomass production rate (g FW m⁻² day⁻¹). Errors shown are ± 1.0 S.E. from linear regression. (c) OER after 28 days, measured at 300 μmol m⁻² s⁻¹ incident light intensity. Errors shown are ± 1.0 S.D., n = 2.

Fig. 8. Images of *O. secundiramea* plantlets on 1.6 mm mesh panel (7 x 7 cm) at inoculation, and after 28 days of cultivation within the aeration tank shown in Fig. 2. (a) Plantlet clusters on 20 mm square pitch; (b) plantlet clusters on 12 mm square pitch; (c) adjacent plantlet clusters at spacing of 8 mm; (d) contiguous layer of plantlets.

Fig. 9. Images of *O. secundiramea* plantlet morphology on mesh panel. (a) Plantlet clusters inoculated at 20 mm pitch after 28 days of cultivation, viewed from the panel edge. (b) Close-up of one plantlet cluster. (c) Contiguous layer of plantlets after 3 days of cultivation, viewed from the panel edge. (d) Contiguous layer of plantlets after 28 days of cultivation, viewed from the panel edge. (e) Close-up of contiguous layer biomass turf.

Fig. 10. Coverage of *O. secundiramea* plantlets on panel surface with time. (a) Fractional coverage; (b) biomass normalized to active area on the mesh, defined as the area on the mesh surface occupied by the shoot tissues. Errors shown are ± 1.0 S.E., $n = 3$.

Fig. 1

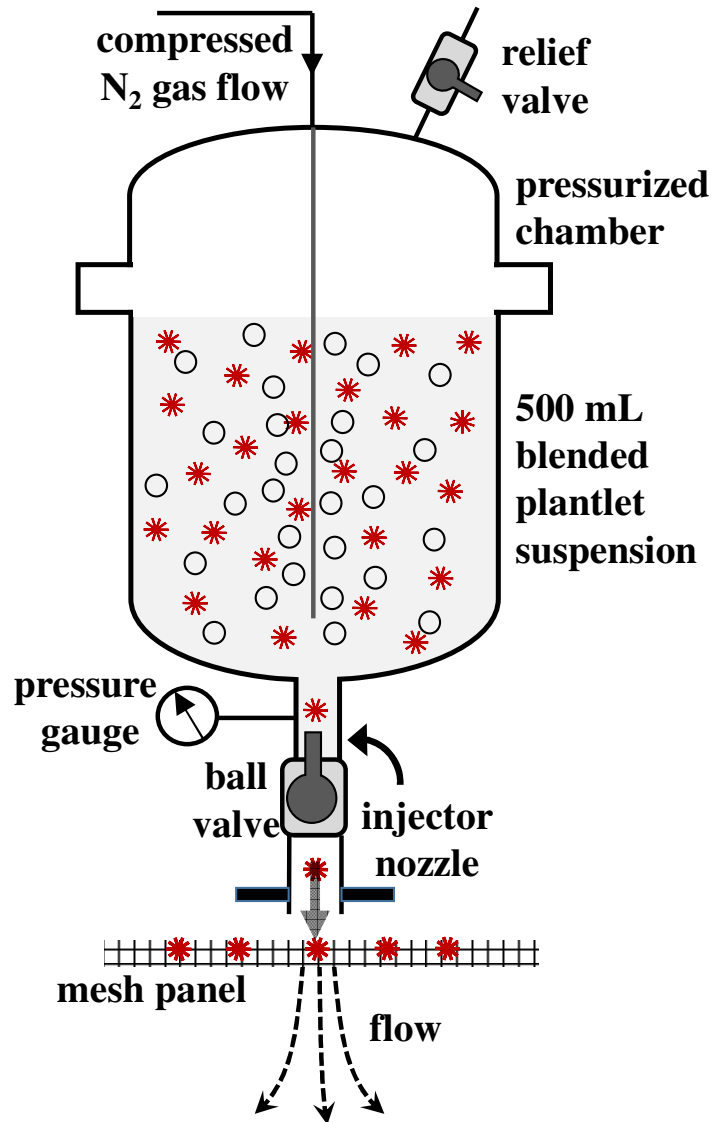


Fig. 2

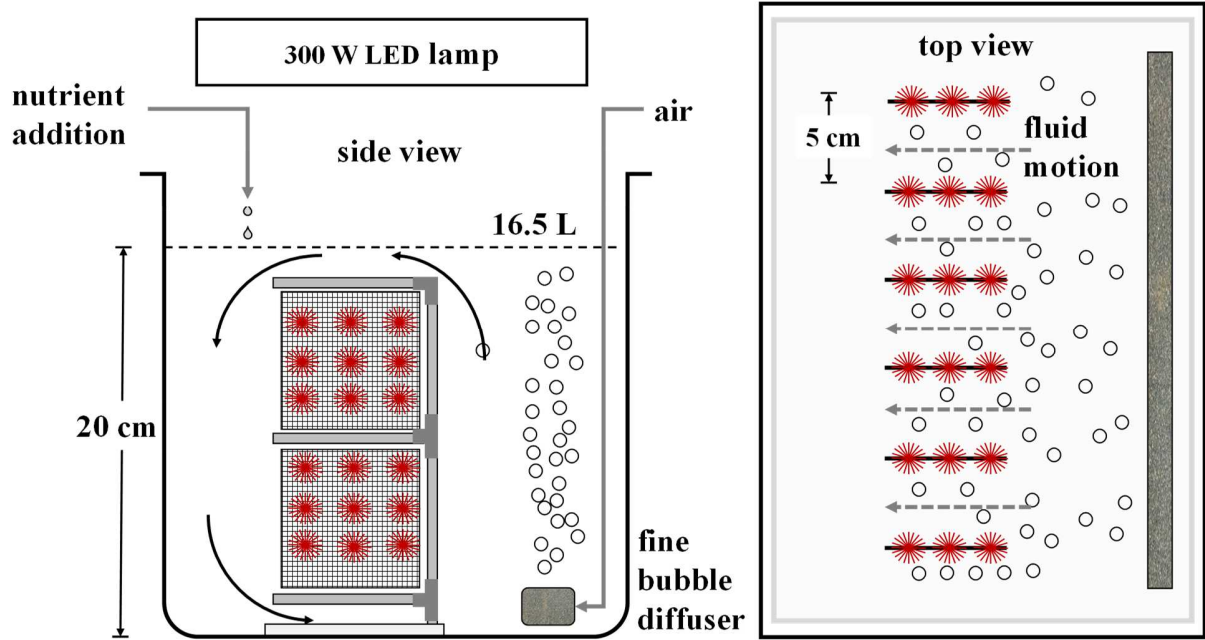


Fig. 3

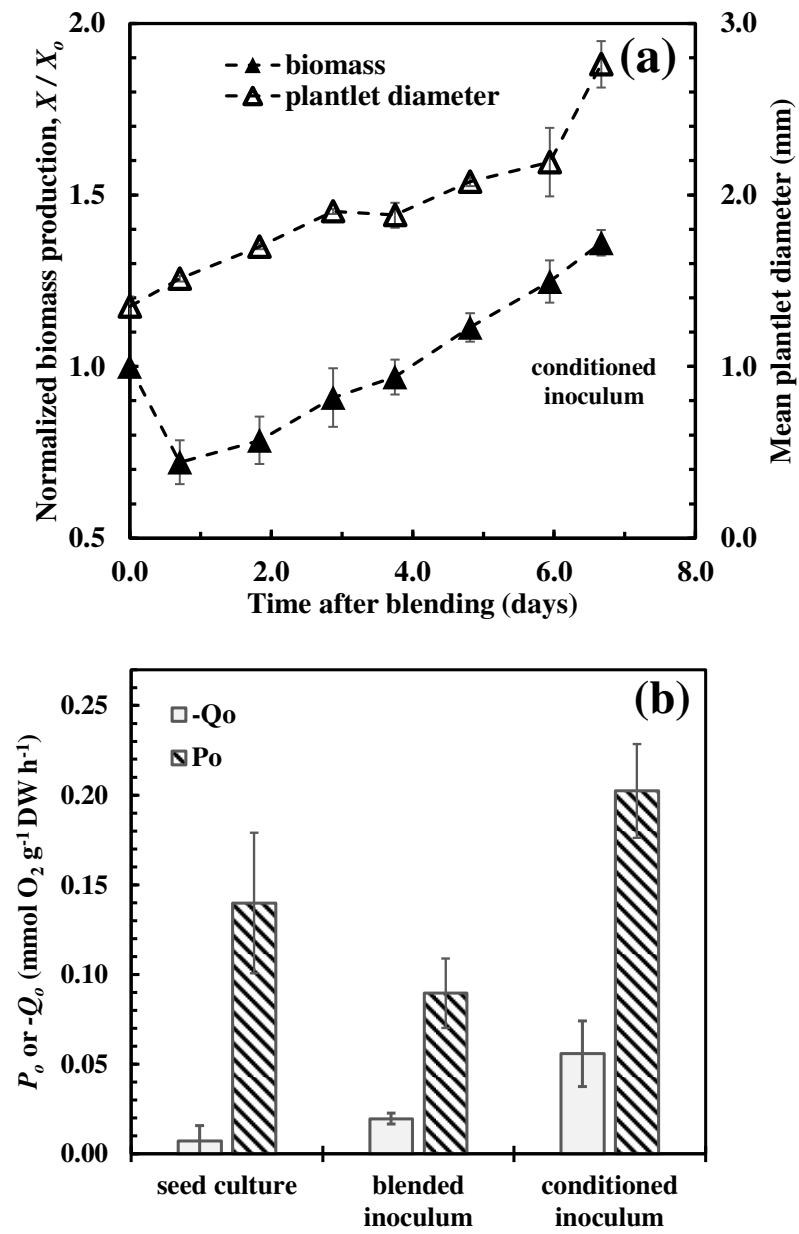


Fig. 4

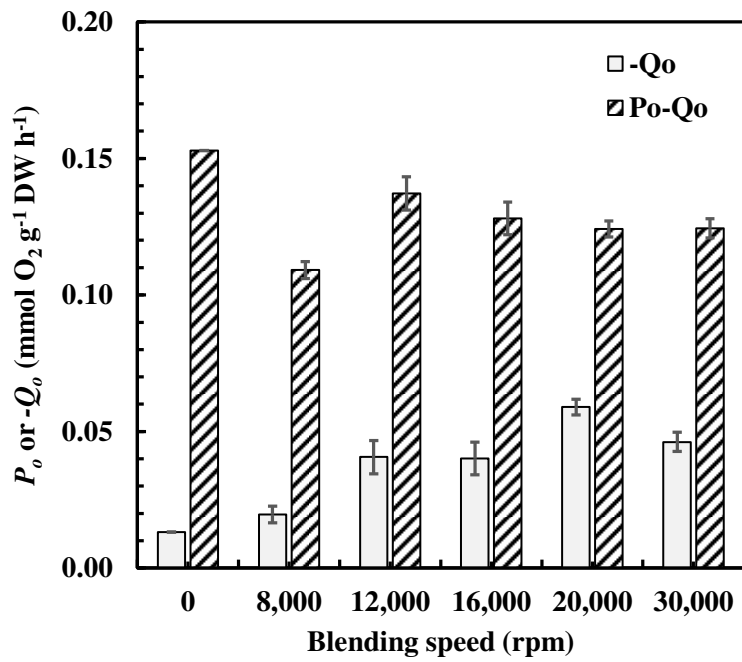


Fig. 5

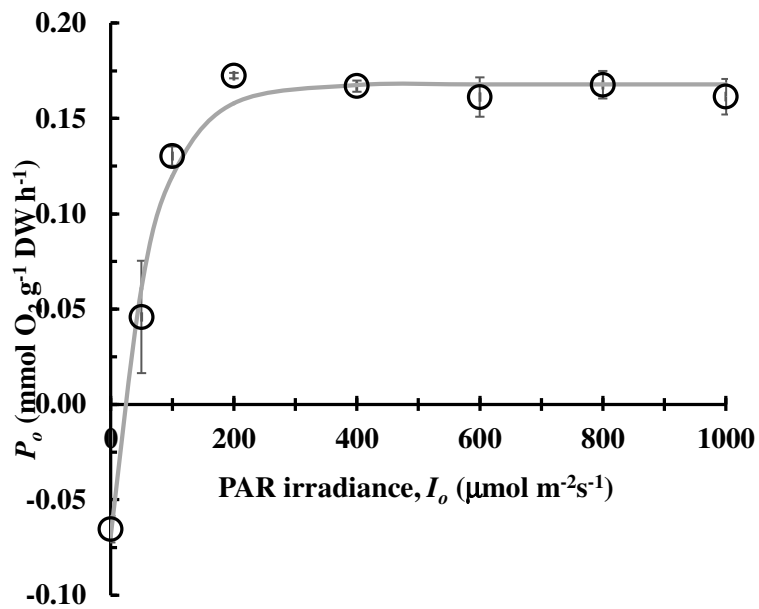


Fig. 6

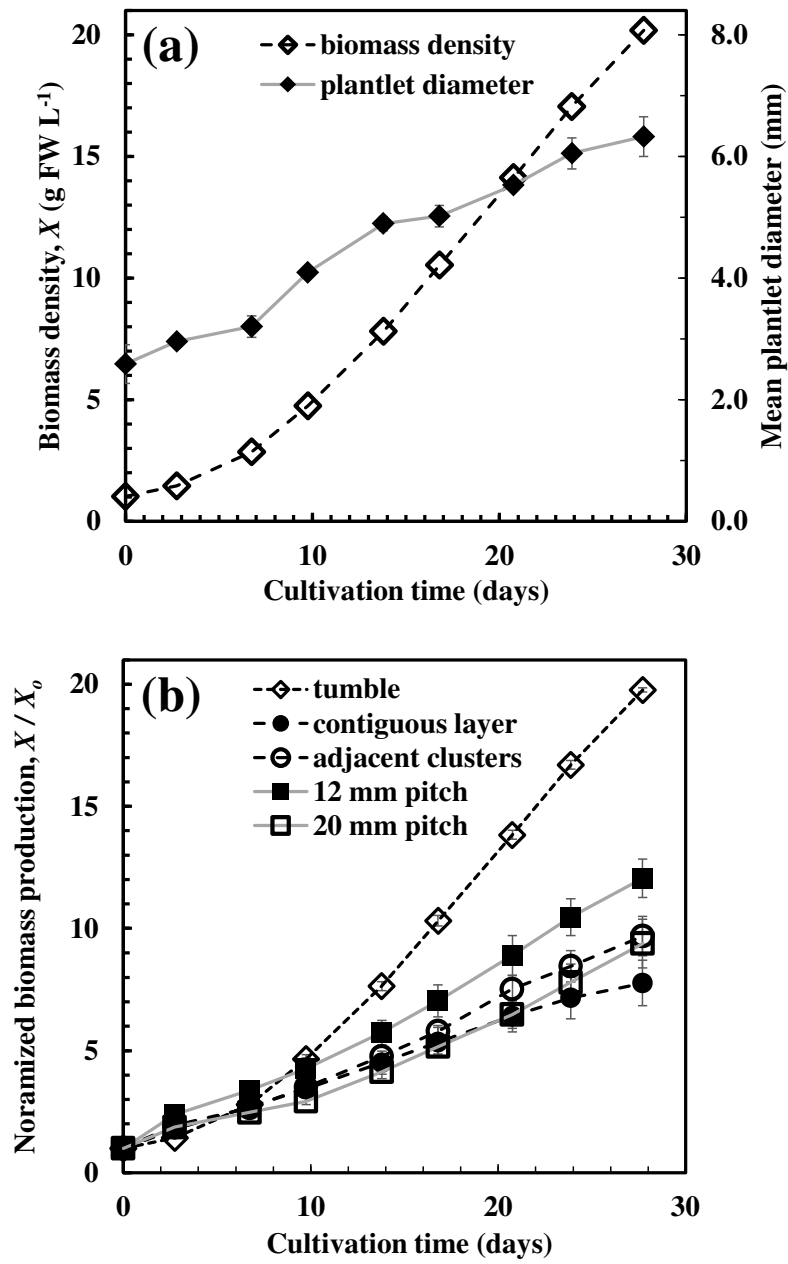


Fig. 7

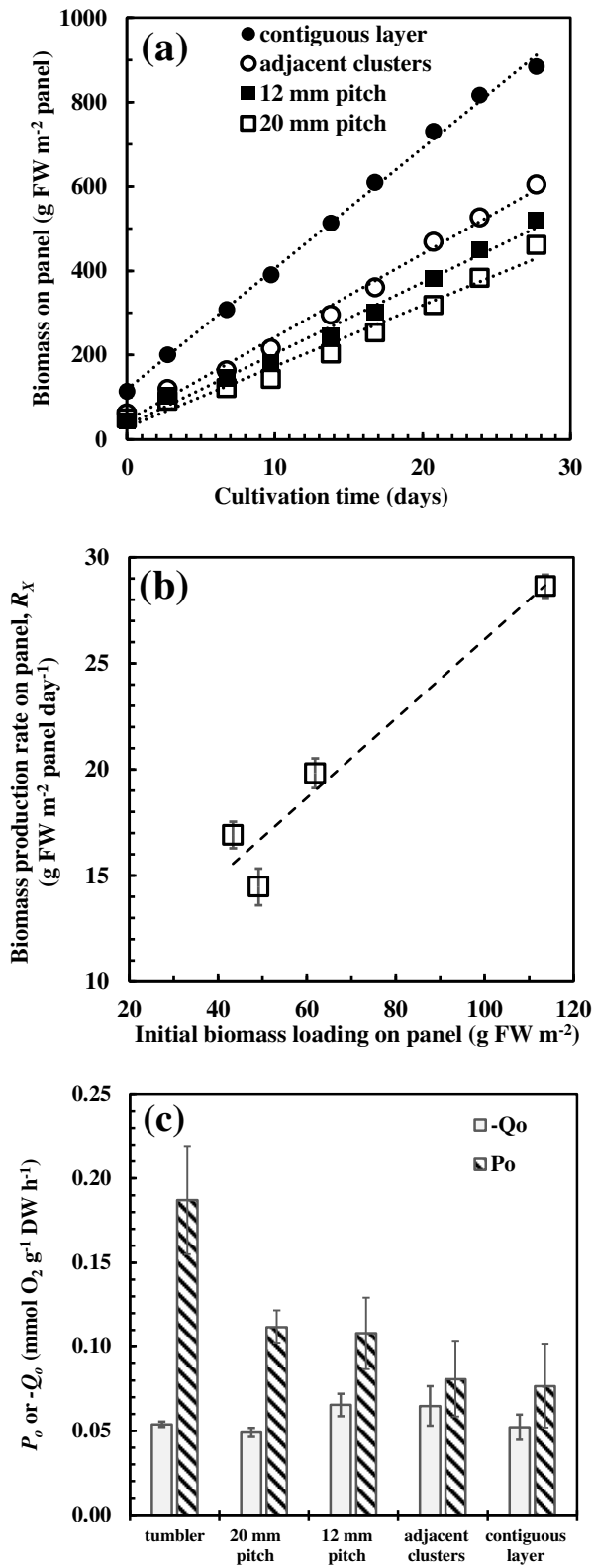


Fig. 8

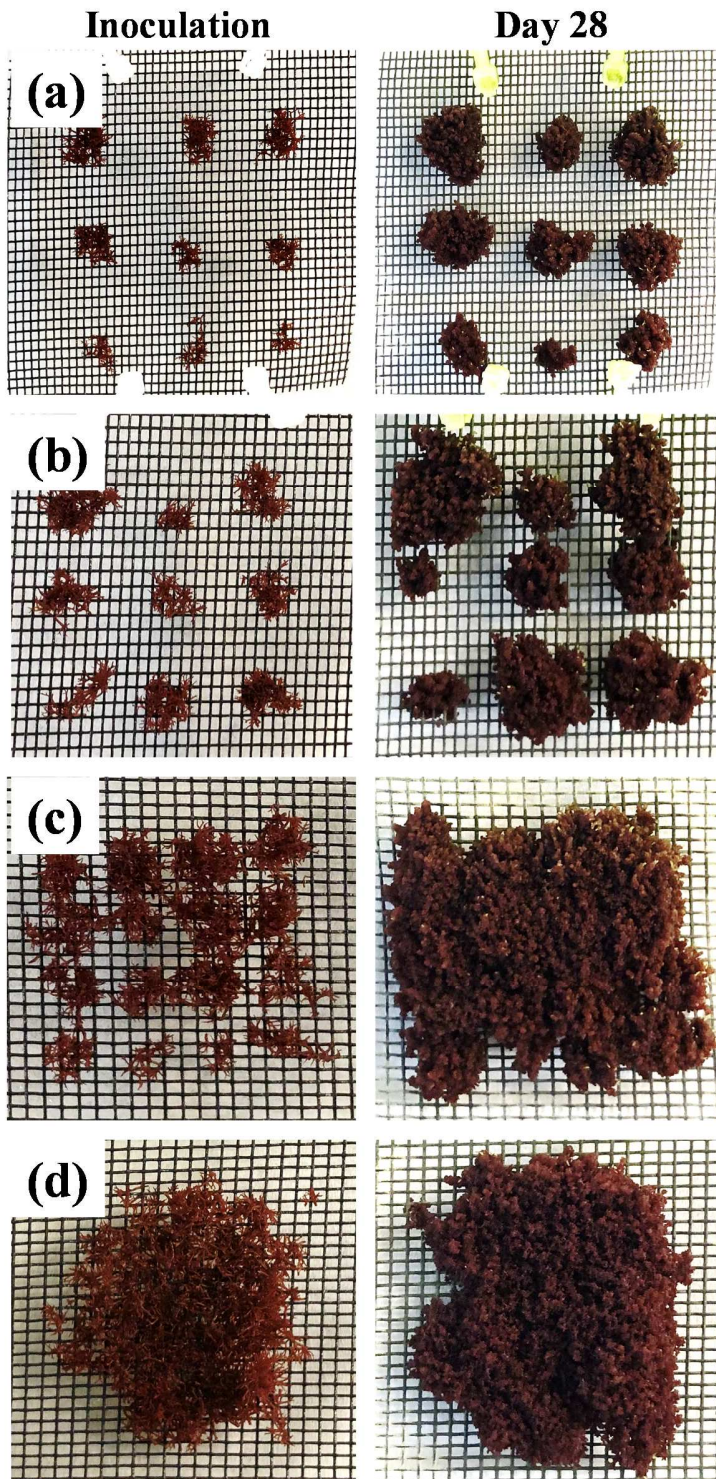


Fig. 9

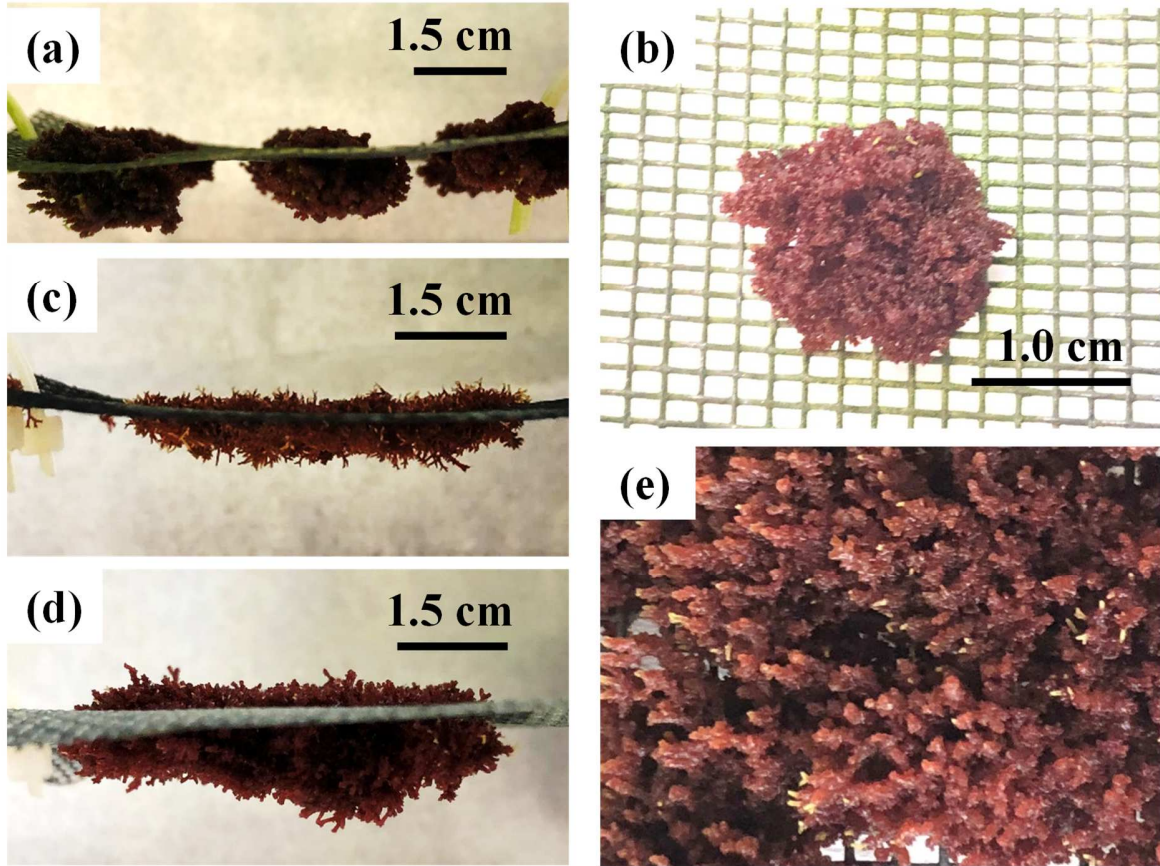


Fig. 10

